Phytopathology Research

RESEARCH

Open Access

Transcriptome and differential expression analysis revealed the pathogenic-related genes in *Magnaporthe oryzae* during leaf and panicle infection

Yan Du[1], Dong Liang[2], Zhongqiang Qi[1], Junjie Yu[1], Rongsheng Zhang[1], Tianqiao Song[1], Mina Yu[1], Huijuan Cao[1], Xiayan Pan[1], Shuchen Wang[1], Junqing Qiao[1], Youzhou Liu[1] and Yongfeng Liu[1*]

Abstract

Magnaporthe oryzae is one of the most destructive pathogens that threaten rice production around the world. Previous studies mainly focus on pathogenic mechanism of *M. oryzae* during infection on rice at leaf stage. However, the pathogenic mechanism of *M. oryzae* infection on panicle tissue is not well understood. In the present study, we performed RNA sequencing (RNA-seq) to study gene expression patterns of *M. oryzae* during infection at leaf stage and at panicle stage, respectively. The differentially expressed genes (DEGs) of *M. oryzae* in the infected leaf and panicle tissues were analyzed. Gene ontology (GO) enrichment analysis of DEGs revealed that *M. oryzae* genes involved in the biological processes were different at leaf and panicle stages. Furthermore, Kyoto Encyclopedia of Genes and Genomes (KEGG) analysis of DEGs indicates that genes related to individual and important pathways may function at different infection stages. In particular, CAZymes carbohydrate esterases (CEs), carbohydrate-binding modules (CBMs), and glycoside hydrolases (GHs) may play important roles during *M. oryzae* infection on rice leaves, while glycosyltransferases (GTs) and GHs may play important roles during infection at rice panicle stage. Further analysis of effectors (*BAS3, BAS113, BAS162, MoCDIP4*, and *MoHEG13*) and their homologous genes suggest that they are involved in host defense suppression. Our findings provide insights into understanding the infection mechanisms of *M. oryzae* for rice leaf blast and panicle blast disease.

Keywords *Magnaporthe oryzae*, Leaf blast, Panicle blast, RNA-sequencing, CAZymes, Effectors

Background

Rice blast disease, caused by the hemibiotroph fungal pathogen *Magnaporthe oryzae*, is one of the most important diseases of rice (*Oryzae sativa*) worldwide. The pathogen causes symptoms on leaves and panicle necks known as leaf and panicle blast, respectively (Khan et al. 2014). In particular, neck blast has major impact on rice yield loss. Although there is a high resistance correlation between leaf blast and panicle blast, leaf blast resistance does not conclusively confer resistance to panicle blast (Ou & Nuque 1963; Balal et al. 1977). Not only the resistance of a given variety to different *M. oryzae* races is different, but also the resistance to the same race may be different at different rice growth stages (Hu et al. 2014; Du et al. 2021b). Therefore, clarifying the distinct infection mechanisms

*Correspondence:
Yongfeng Liu
liuyf@jaas.ac.cn
[1] Institute of Plant Protection, Jiangsu Academy of Agricultural Science, Nanjing 210014, China
[2] College of Advanced Agricultural Sciences, Zhejiang A&F University, Zhejiang 311300, China

of *M. oryzae* on rice at leaf and panicle stages will help better understand the interactions between rice and *M. oryzae*.

Phytopathogenic fungi can be classified into two types: those infecting plant leaves and stems and those proliferating in root tissues (Agrios 1997). Infection of these tissues and the subsequent survival within them require distinct strategies. Previous research showed that *M. oryzae* mutant strains lacking karyopherin exportin-5 (*EXP5*) gene were much less virulent on plant roots revealed an important function of EXP5 during *M. oryzae* colonization of underground plant tissues (Tucker et al. 2010). For leaf tissue infection, *M. oryzae* has emerged as a paradigm for molecular genetic dissection of factors that determine fungal pathogenicity on plant leaves. Mutational analyses have identified a number of genes in *M. oryzae* that are required for its colonization of leaf tissue (Dean et al. 2005; Oh et al. 2008; Mehrabi et al. 2009; Kong et al. 2013). So far, more than 1600 genes in *M. oryzae* have been investigated by targeted gene deletion or mutagenesis, covering over 10% of the genome (Yan et al. 2023). However, it is not well known about the factors that are required for successful colonization on neck tissues, despite the importance of neck blast.

RNA sequencing (RNA-seq) is a useful and affordable method to analyze gene expression patterns for either pathogen or host during infection, and helps understand host and pathogen interaction. Transcriptomes enable us to reveal infection-specific expression of *M. oryzae* genes in leaf and neck tissues (Mosquera et al. 2009; Soanes et al. 2012; Shimizu et al. 2019; Jeon et al. 2020). Recently, Mahesh et al. 2021 reported several *M. oryzae* pathogenicity genes related to tissue specificity during rice-*Magnaporthe* interactions by transcriptome analysis, resulting in the identification of 439 genes that were specifically expressed in neck-infected fungus, with 360 of them being hypothetical proteins (Mahesh et al. 2021). Of the identified genes, mitochondrial chaperone BCS1 (MGG_13867), secretory lipase (MGG_14628), cutinase (MGG_01943), ferric reductase transmembrane component (MGG_02828), endo-1,4-beta-xylanase B (MGG_08331), fungal cellulose binding domain-containing protein (MGG_01403), glycine cleavage system T protein (MGG_04826), 2-(R)-hydroxylpropyl-CoM dehydrogenase (MGG_12982), GPI inositol-deacylase (MGG_01844), and chitin deacetylase (MGG_05828) were more than 40-fold up-regulated in rice neck infecting fungus. Sixteen genes were specifically expressed in leaf-infecting fungus and most of them were hypothetical proteins (Mahesh et al. 2021). However, there are few reports on infection expression related genes in *M. oryzae* that are specific expressed during the infection on rice panicle stage. Therefore, research on the expression profile of *M. oryzae* upon infection in leaf and neck could help understand the epidemics of blast disease.

In this study, transcriptomes of *O. sativa* L. ssp. *japonica* cv. 'Nipponbare' (Nip) inoculated with *M. oryzae* GUY-11 was used to compare gene expression profiles of *M. oryzae* during leaf and neck infection stages at 8, 24, and 48 h post-inoculation (hpi). Our objective aims to analyze the differentially expressed genes of *M. oryzae* between the infection on rice at leaf and neck stages, and to identify potential genes may serve as fungicide targets for rice blast control in future.

Results

Transcriptome sequencing and data analysis

To study the differential regulation of *M. oryzae* during the infection on rice leaf and panicle, the conidia of *M. oryzae* strains GUY-11 were used to inoculate the plants. The inoculated leaf and panicle tissues of rice variety Nipponbare (Nip) were collected at 8, 24, and 48 hpi, respectively. Nip leaf and panicle tissues inoculated with sterile distilled water were defined as control samples leaf-CK (L-CK) and panicle-CK (P-CK) (Fig. 1). Total RNA of leaf and panicle tissues was extracted, and RNA-seq of the collected samples was performed. Approximately 68 to 80 million pairs of reads from each sample were used in the downstream analysis. All clean reads were mapped to the reference genome of *M. oryzae* 70-15 (Genebank accession No. GCA_000002495.2). An overview of the mapped statistics is provided (Table 1).

The differentially expressed genes in *M. oryzae* during infection on rice leaf and neck tissues

The differentially expressed genes (DEGs) were identified with adjusted p-values < 0.01 and at least a 1.5-fold change in the normalized Fragments Per Kilobase of exon model per Million mapped fragments (FPKM) expression values. We compared transcriptome profile of *M. oryzae* from infected leaf and panicle at 8, 24, and 48 hpi, using the transcriptome of *M. oryzae* conidia as a control. There were 440 genes (283 up-regulated and 157 down-regulated), 737 genes (576 up-regulated and 161 down-regulated), 877 genes (628 up-regulated and 249 down-regulated) were differentially expressed in leaf infection stage compared to conidia (control), respectively. Meanwhile, there were 1432 genes (760 up-regulated and 672 down-regulated), 3355 genes (1891 up-regulated and 1464 down-regulated), 4528 genes (2425 up-regulated and 2103 down-regulated) were differentially expressed in *M. oryzae* during infection on panicle (Fig. 2a, b and Additional file 1: Table S1). The comparison of *M. oryzae* genes indicated that 333 genes were common, and these genes were both differentially expressed at L8 and P8 stages compared to conidia.

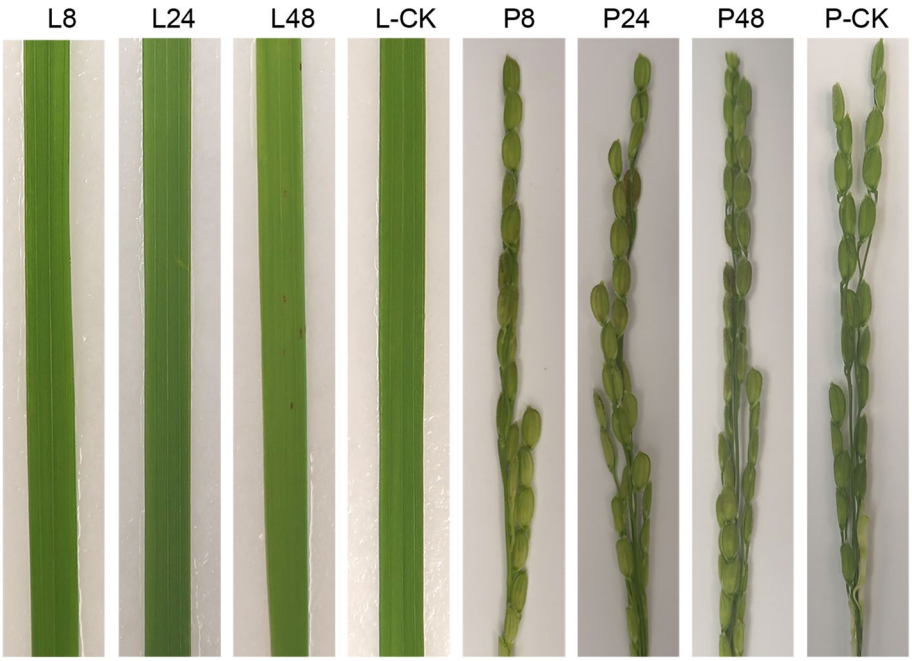

Fig. 1 Leaf and panicle tissue samples were collected at 8, 24, and 48 hpi, respectively. Leaf and panicle tissues were inoculated by conidia suspension (1×10^5 conidia/mL). Leaf and panicle were inoculated by sterile distilled water as blank control (L-CK and P-CK)

Table 1 Summary of alignment statistics in 19 libraries referring to *Magnaporthe oryzae* 70-15 genome

Sample	Total Reads	Mapped Reads	Uniq Mapped Reads	Multiple Map Reads	Reads Map to '+'	Reads Map to '-'
L8-1	71,950,078	82,241 (0.11%)	81,832 (0.11%)	409 (0.00%)	41,452 (0.06%)	41,553 (0.06%)
L8-2	77,327,364	84,133 (0.11%)	83,747 (0.11%)	386 (0.00%)	42,443 (0.05%)	42,555 (0.06%)
L8-3	64,235,308	52,803 (0.08%)	52,566 (0.08%)	237 (0.00%)	26,647 (0.04%)	26,676 (0.04%)
L24-1	69,979,766	101,355 (0.14%)	99,689 (0.14%)	1,666 (0.00%)	52,023 (0.07%)	52,016 (0.07%)
L24-2	69,118,726	77,567 (0.11%)	76,452 (0.11%)	1,115 (0.00%)	39,612 (0.06%)	39,670 (0.06%)
L24-3	66,222,534	76,750 (0.12%)	75,674 (0.11%)	1,076 (0.00%)	39,116 (0.06%)	39,276 (0.06%)
L48-1	75,255,820	74,258 (0.10%)	71,951 (0.10%)	2,307 (0.00%)	38,991 (0.05%)	38,951 (0.05%)
L48-2	76,639,570	111,855 (0.15%)	108,721 (0.14%)	3,134 (0.00%)	58,333 (0.08%)	58,367 (0.08%)
L48-3	811,299,04	115,727 (0.14%)	113,567 (0.14%)	2,160 (0.00%)	59,503 (0.07%)	59,534 (0.07%)
P8-1	857,234,38	249,117 (0.29%)	247,546 (0.29%)	1,571 (0.00%)	125,799 (0.15%)	126,053 (0.15%)
P8-2	698,014,74	176,570 (0.25%)	175,522 (0.25%)	1,048 (0.00%)	89,107 (0.13%)	89,223 (0.13%)
P8-3	85,822,380	256,131 (0.30%)	254,544 (0.30%)	1,587 (0.00%)	129,364 (0.15%)	129,607 (0.15%)
P24-1	90,825,004	692,916 (0.76%)	688,041 (0.76%)	4,875 (0.01%)	349,960 (0.39%)	350,555 (0.39%)
P24-2	72,218,216	580,096 (0.80%)	574,770 (0.80%)	5,326 (0.01%)	294,438 (0.41%)	294,759 (0.41%)
P24-3	77,204,686	582,877 (0.75%)	578,906 (0.75%)	3,971 (0.01%)	294,327 (0.38%)	294,344 (0.38%)
P48-1	68,303,350	1,228,797 (1.80%)	1,210,705 (1.77%)	18,092 (0.03%)	629,462 (0.92%)	629,701 (0.92%)
P48-2	73,796,272	731,808 (0.99%)	719,842 (0.98%)	11,966 (0.02%)	375,398 (0.51%)	376,149 (0.51%)
P48-3	100,185,108	2,457,397 (2.45%)	2,420,003 (2.42%)	37,394 (0.04%)	1,260,573 (1.26%)	1,262,790 (1.26%)
Conidia	45,664,514	43,459,652 (95.17%)	43,058,316 (94.29%)	401,336 (0.88%)	22,332,816 (48.91%)	22,358,931 (48.96%)

Reads Map to '+': Number of Reads aligned to the positive strand of the reference genome and their percentage in clean reads

Reads Map to '-': Number of Reads aligned to the negative strand of the reference genome and their percentage in clean reads

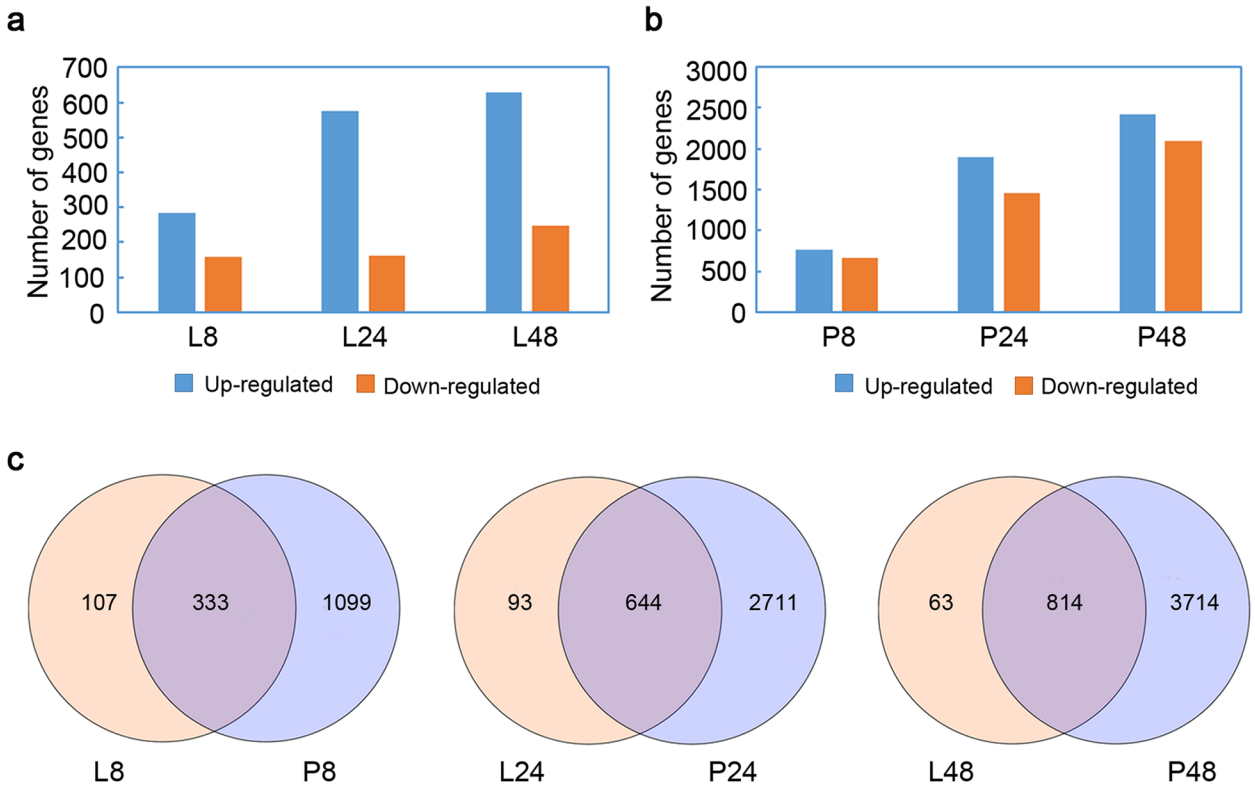

Fig. 2 Overview of differentially expressed genes (DEGs) identified in *M. oryzae* at the initial stages of leaf and panicle. **a**, **b** The number of differently expressed genes at L8, L24, and L48, and P8, P24, and P48. **c** Venn diagram showing commonly and specifically expressed genes in *M. oryze* at leaf and panicle infection stages. L8, L24, and L48 are leaf-infected samples. P8, P24, and P48 are panicle-infected samples

There were 107 genes differentially expressed compared to conidia at L8 but not at P8 stage and 1099 genes were differentially expressed at P8 but not at L8 stage. At 24 h, 644 were common between L24 and P24 stage, 93 and 2711 genes were differentially expressed at L24 and P24 stage, respectively. Similar analysis indicated that 814 genes at 48 hpi were shared between L48 and P48 stage, 63 and 3714 genes were differentially expressed at L48 and P48 stages, respectively (Fig. 2c, Additional file 2: Table S2, and Additional file 3: Table S3). Venn diagram analysis showed that *M. oryzae* genes are differentially expressed at the stages of leaf and panicle infection.

Gene ontology enrichment analysis of the DEGs

To investigate the underlying mechanisms in *M. oryzae* during the two infection stages, GO classification of DEGs at 8, 24, and 48 hpi was analyzed. The results of GO enrichment analysis of *M. oryzae* DEGs are provided in Additional file 4: Table S4 and Additional file 5: Table S5. Go terms were visualized in biological process, cellular component, and molecular function categories, which revealed the GO functional classification of DEGs (Fig. 3). A comparison of the number of three GO terms showed that GO terms at L8 (10, 11, 5) and P8 (16, 13, 11) were enriched in biological process, cellular component, and molecular function categories, respectively. Similarly, GO terms at L24 (6, 9, 4) and P24 (17, 13, 12) were enriched in these three categories, as GO terms at L48 were 8, 7, 4, and P48 were 18, 14, 16 in these three categories. Notably, the number of GO terms at panicle infection stages was greater than that at leaf infection stages. Further analysis revealed that DEGs at panicle infection stage (P8, P24, and P48) were significantly enriched in biological process, like "metabolic process", "cellular process", and "single-organism process". Additionally, DEGs analysis demonstrated significant enrichment in cellular component, including "membrane", "membrane part", "cell", and "cell part". Furthermore, the molecular functions "catalytic activity" and "binding" were also significantly enriched among these DEGs. Overall, it is evidence that *M. oryzae* DEGs at panicle infection stage may be involved in more important functional processes than leaf infection stage.

Pathway analysis of the DEGs in *M. oryzae*

For pathway analysis, we mapped all DEG with more than 1.5-fold differential representation to terms in the Kyoto Encyclopedia of Genes and Genomes (KEGG) database,

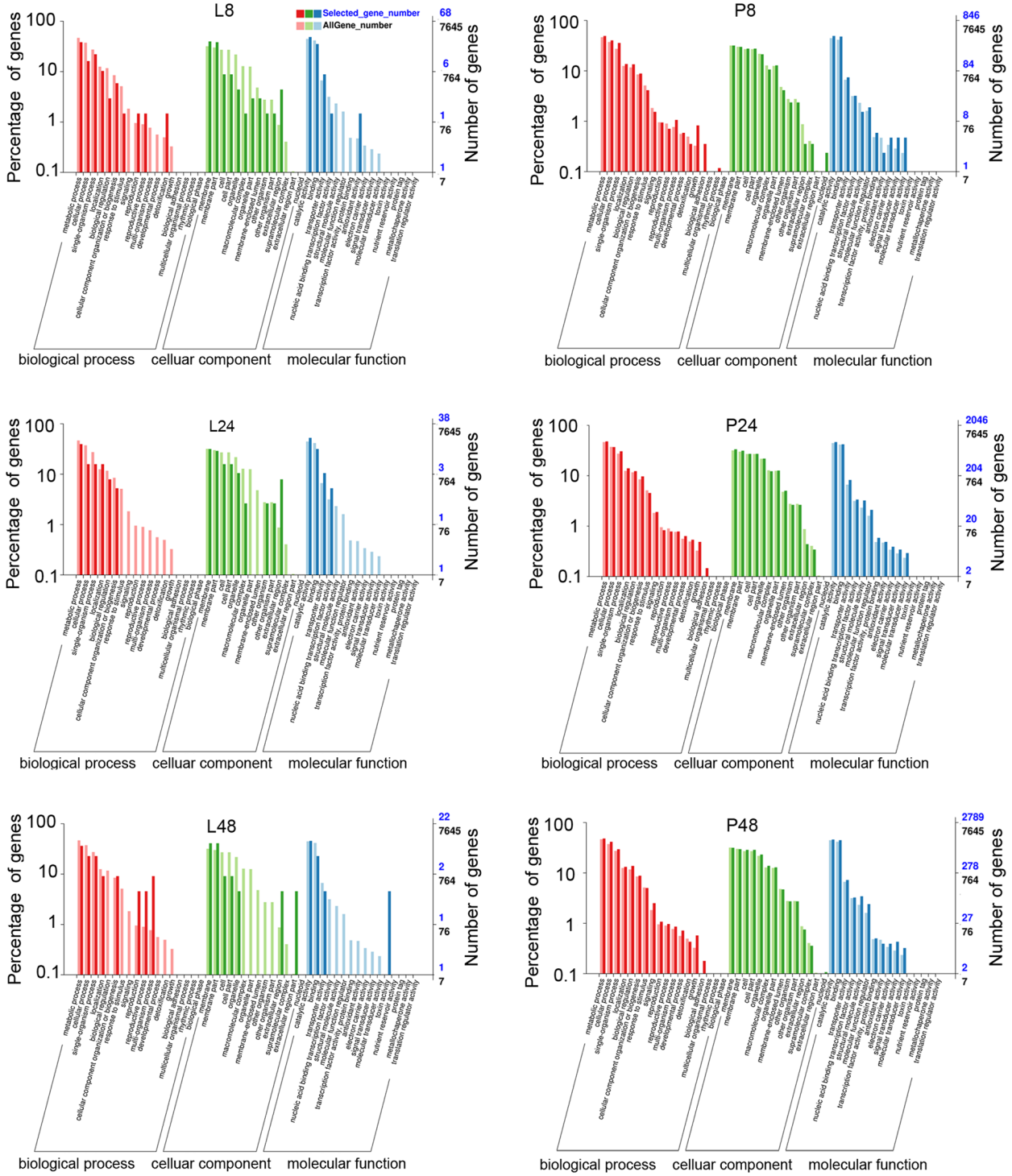

Fig. 3 GO classification of differentially expressed genes in *M. oryzae* at different leaf and panicle infection stages

and then searched significantly enriched pathway terms against the genome annotation. To perform functional classification and pathway assignment of genes that are activated in *M. oryzae*, DEGs in each comparison were mapped with the KEGG database. For the leaves at 8, 24, and 48 hpi, the KEGG enrichment pathways of 107, 93, and 63 DEGs were analyzed (Additional file 2: Table S2). We found 4 DEGs at 8 hpi were enriched in "amino sugar

and nucleotide sugar metabolism" pathways, and 3, 2, 2, 2 DEGs at 24 hpi were enriched in "Biosynthesis of amino acids", "ABC transporters", "Cysteine and methionine metabolism", and "Glyoxylate and dicarboxyolate metabolism" pathways, respectively, and 2 DEGs at 48 hpi were enriched in "Glutathione metabolism" pathways (Fig. 4 and Additional file 6: Table S6). However, many DEGs at panicle infection stage exhibited different pathways. For panicle infection at 8, 24, and 48 hpi, there are 1099, 2711, and 3714 DEGs analyzed based on KEGG enrichment (Additional file 3: Table S3). We found that DEGs were mainly enriched in "Carbon metabolism" pathway from 8 h (36 genes) to 24 h (64 genes) post inoculation, In addition, DEGs were mainly enriched in "Ribosome" pathway from 24 h (54 genes) to 48 h (79 genes) post inoculation (Fig. 4 and Additional file 6: Table S6). The results suggest that *M. oryzae* genes related to these pathways may perform individual and important functions on leaf and panicle infection stages.

Analysis of *M. oryzae* carbohydrate-active enzymes during leaf and panicle infection

Phytopathogenic fungi produce cell wall degrading enzymes (CWDEs) to breach the plant cell wall, which is the most important physical barrier during plant-pathogen interaction (Quoc & Chau 2017; Yang et al. 2021). Carbohydrate-active enzymes (CAZymes) are involved in the metabolism of glycoconjugates, polysaccharides, and oligosaccharides. For plant pathogens, CAZymes help in the degradation of the host cell wall and storage compounds (Zerillo et al. 2013). According to their functions, CAZymes can be classified into glycoside hydrolases (GHs), glycosyltransferases (GTs), polysaccharide lyases (PLs), carbohydrate esterases (CEs), auxiliary activities (AAs), and carbohydrate-binding modules (CBMs) (http://www.cazy.org/). We predicted CAZymes of *M. oryzae* using the dbCAN web server 2 (Yin et al. 2012), HMMER (Finn et al. 2011), and DIAMOND (Buchfink et al. 2015), in which we identified CAZymes-coding genes for DEGs at the leaf infection and panicle infection stages. Subsequently, we found that most DEGs related to CAZymes in *M. oryzae* were obviously increased from at least 2-fold to 100-fold expression levels at leaf infection stage. At L8, the expression levels of *M. oryzae* CE5 subfamily genes (MGG_14095, MGG_02393, MGG_09100, MGG_03440), GH subfamily genes (MGG_05533, MGG_11231, MGG_01885, MGG_09733, MGG_01096), CBM subfamily genes (MGG_03857, MGG_07264), and AA subfamily

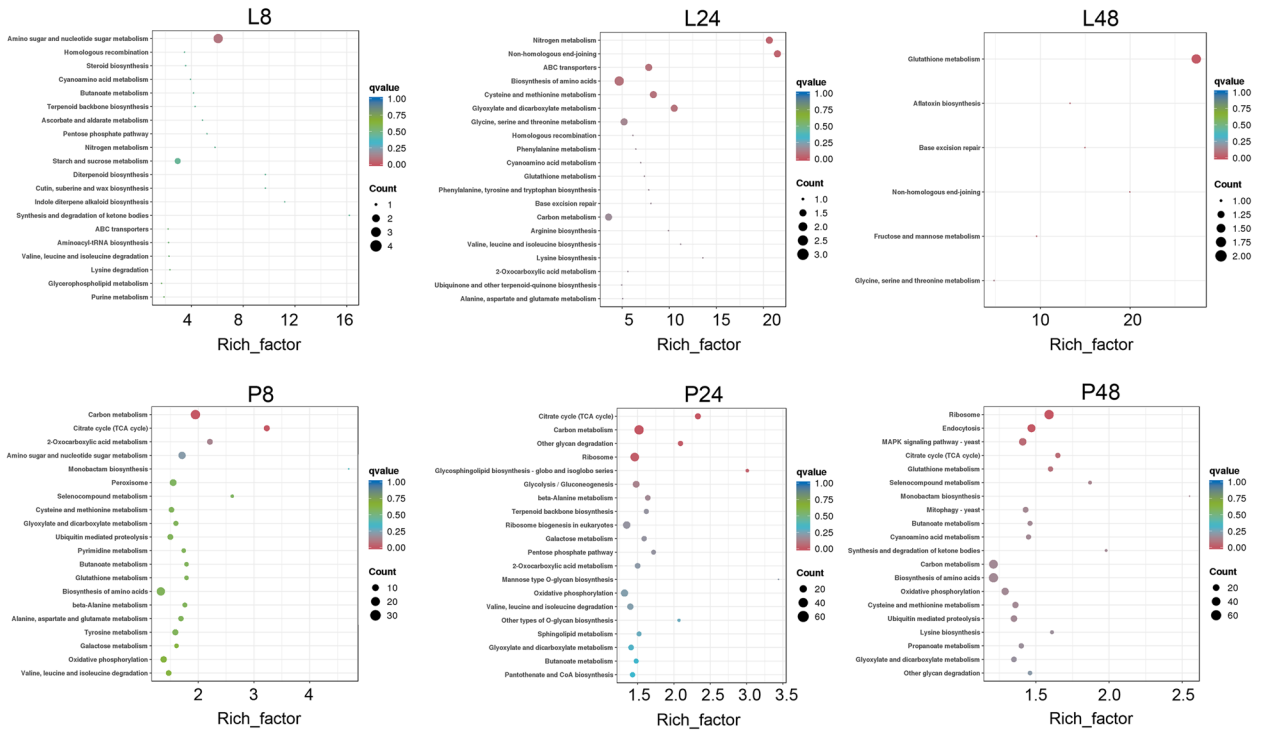

Fig. 4 Enrichment factor scatter plot of significant KEGG pathways in *M. oryzae* at different leaf and panicle infection stages. The horizontal axis represents rich factors, and the vertical axis represents metabolic pathways. The location of bubbles represents the enrichment item, the size of bubbles represents the number of differential genes, and the color of bubbles represents the significant degree of enrichment

genes (MGG_14940, MGG_01255) were significantly increased compared to P8 stage. Similarly, the expression levels of *M. oryzae* CE4 subfamily gene (MGG_14966), CE8 subfamily gene (MGG_14400), CE5 subfamily genes (MGG_15403, MGG_11966, MGG_09100), GH10 subfamily gene (MGG_01542), AA9 subfamily gene (MGG_07575) were significantly increased compared to panicle infection at 24 hpi. For leaf infection at 48 hpi, the expression levels of GH18 subfamily gene (MGG_05125) and GT2 subfamily gene (MGG_07803) were slightly increased (Fig. 5a and Additional file 7: Table S7). Overall, CE, GH, and CBM families may function in the degradation of plant cuticles at the leaf infection stage.

For panicle infection stage, most DEGs belong to GT and GH families. We found that fifteen DEGs were common in panicle-infected fungus (Additional file 8: Table S8), and these genes belong to GT subfamily (MGG_03860, MGG_04773, MGG_03185, MGG_00865, MGG_06064, MGG_13971, MGG_02954, MGG_01802, MGG_08182), and GH subfamily (MGG_00063, MGG_00316, MGG_04765, MGG_13455, MGG_02793, MGG_07101), which may be conserved during panicle infection stage. Besides, some genes belonged to GH subfamily were also found differentially and specifically expressed at panicle infection stage. These genes were significantly upregulated about 2-fold to 50-fold at individual panicle infection stage (Fig. 5a and Additional file 8: Table S8). The CAZymes for DEGs at 8 hpi included GH18 subfamily (MGG_17153), GT subfamily (MGG_01140, MGG_02384, MGG_03441, MGG_07289, MGG_13014), and those DEGs at 24 hpi included PL4_3 subfamily (MGG_06041), GT subfamily (MGG_00636, MGG_04979, MGG_07230), GH subfamily (MGG_00084, MGG_00677, MGG_05533, MGG_06023, MGG_07634, MGG_07715, MGG_11475, MGG_17864). DEGs related to CAZymes at 48 hpi mainly are GT subfamily (MGG_07979, MGG_05687, MGG_04145, MGG_06137, MGG_02859, MGG_03459, MGG_04514, MGG_07729, MGG_14118, MGG_09962), GH subfamily (MGG_02793, MGG_14903, MGG_11536, MGG_01885, MGG_00667, MGG_11210, MGG_10712, MGG_14954, MGG_05520, MGG_04689, MGG_07101, MGG_06834, MGG_03599, MGG_01912, MGG_13455, MGG_11408, MGG_09471). To confirm the expression pattern of DEGs obtained from RNA-seq analysis, six genes were selected randomly and evaluated by quantitative Real-time PCR (qRT-PCR) (Fig. 5b). Comparison of Log_2 fold change values of these genes in RNA-seq and qRT-PCR revealed similarity of gene expression profiles. Taken together, GT and GH families may play aimportant roles at rice panicle infection stage.

M. oryzae effectors were differentially expressed during leaf and panicle infection

During infection, *M. oryzae* secretes a set of effectors to disturb plant immune systems (van der Does & Rep 2007; Oliva et al. 2010). In addition to suppress plant immunity, effectors may target cell signaling and metabolic pathways to facilitate invasive fungal growth (van der Does & Rep 2007). Many *M. oryzae* effectors are recognized by rice immune receptors, leading to disease resistance (Yan et al. 2023). In this study, 46 known *M. oryzae* effectors were retrieved from previous study (Gómez Luciano et al. 2019). The hierarchical clustering (HCL) generated a global view of the expression level for verified *M. oryzae* effectors at six time points. As shown in Fig. 6a, most known *M. oryzae* effector genes were highly expressed at both leaf and panicle infection stages, such as *BAS* (*1–4*), *MSP1*, *PWL2*, *SLP1*, *AVR-Pita1*, *AVR-Pia*, *AvrPi9*, and *MC69*. Therefore, these *M. oryzae* conserved effectors are co-regulated during rice infection.

To find homologous effector-encoding genes in the DEGs, the BLASTP toolkit (E-value threshold: $1e^{-15}$) and MCL software (inflation threshold: 4.0) were used to cluster *M. oryzae* genes based on their protein sequences. As shown in Additional file 9: Table S9, *BAS2*, *BAS3*, *BAS113*, *BAS162*, *MoCDIP4*, and *MoHEG13* were found to have different numbers of homologous genes. Based on the FPKM expression values of *M. oryze* effectors and homologous genes at L8, L24, L48, P8, P24, and P48 stages, *M. oryzae BAS2* homologous gene MGG_07749 was increased more than 20-fold at P8 stage compared to L8 stage, and *BAS3* homologous gene MGG_16415 also was increased about 6-fold to 50-fold at panicle infection stage. Similarly, *BAS113* homologous gene MGG_17302 was significantly increased about 8-fold at L24 stage compared to P24 stage. Besides, *MoCDIP4* homologous gene MGG_04547, MGG_07300, and MGG_07686 were significantly increased about 10-fold to 40-fold at P24 and P48 stages. Interestingly, *MoHEG13* (MGG_09378) and its homologous gene MGG_17582 both exhibited higher expression levels at leaf infection and panicle infection stages, but their homologous gene MGG_17319 only exhibited higher expression level at L8 stage compared to P8 stage (Fig. 6a and Additional file 9: Table S9). qRT-PCR was further used to validate RNA-seq results by randomly selecting *M. oryzae* effectors and homologous genes at the early stages of leaf and panicle infection (8, 24, and 48 hpi). The Log_2 fold change values of these genes in RNA-seq and qRT-PCR displayed similar expression profiles (Fig. 6b). The results show that some homologous genes were differentially expressed during leaf and panicle infection stages, indicating that these homologous genes may paly potential roles at different infection stages.

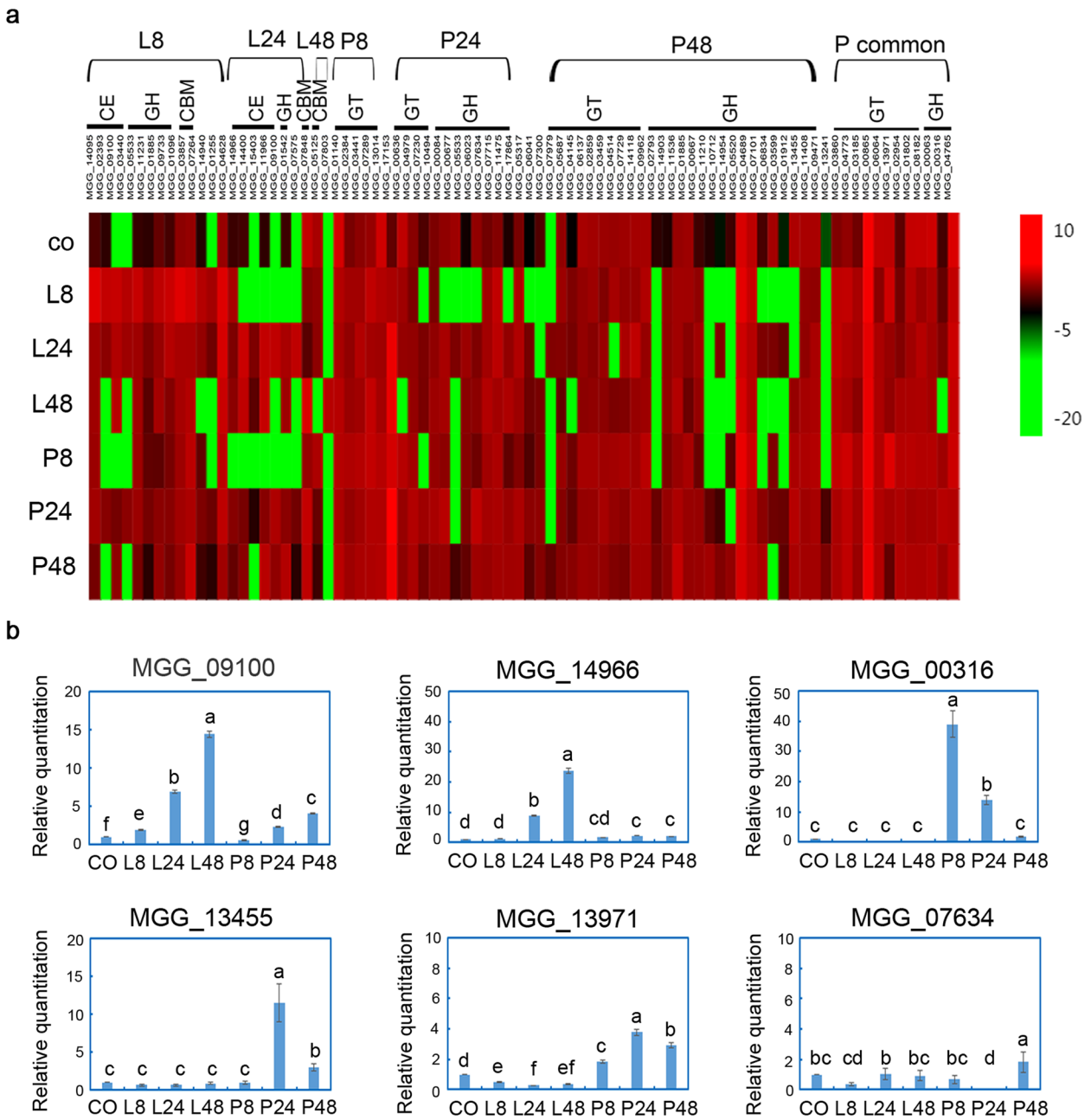

Fig. 5 Differential expression patterns of CAZymes genes of *M. oryzae* during leaf and panicle infection stages. **a** Heatmap showing RNA-seq expression level of CAZymes in *M. oryzae* and panicle during infection on leaf. Normalized FPKM expression are shown in the heatmap. Value of each sample represents the average of normalized FPKM of three replications. Low expression of genes is shown in green rectangle and high expression is shown in red rectangle. L8, L24, L48 represented differential CAZymes genes at leaf stages compared to P8, P24, P48, respectively. P8, P24, P48 represent differential CAZymes genes at panicle stages compared to L8, L24, L48, respectively. P common represented these CAZymes genes are all differential at three panicle stages compared to leaf stages. **b** qRT-PCR was used to verify the expression levels of randomly selected CAZymes genes. The different letters denote significant differences with $P < 0.05$. L8, L24, and L48 represent leaf-infected samples. P8, P24, and P48 are panicle-infected samples, respectively

Discussion

The differences between leaf infection and panicle infection (dual epidemics) are foremost important to understand the molecular interplays for rice-pathogen interactions, which may help to effectively manage the disease. Previous studies mainly focused on infection mechanism of *M. oryzae* on leaf tissue. However, there are little researches on the infection mechanism

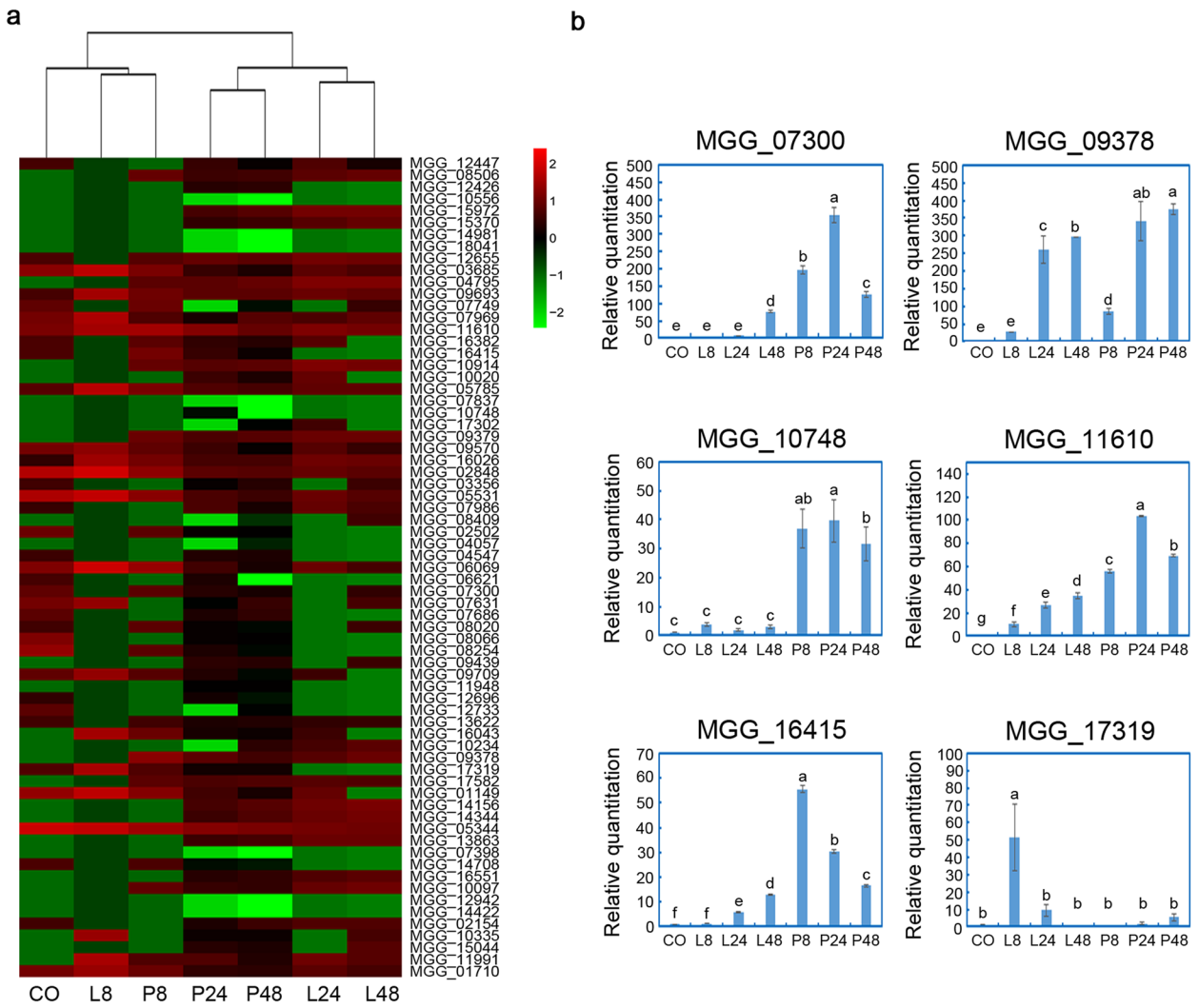

Fig. 6 Differential expression pattern of effector genes in *M. oryzae* during leaf and panicle infection stages. **a** Heatmap showing RNA-seq expression level of verified effector genes and their homologue genes in *M. oryzae* during leaf and panicle interaction. Normalized FPKM expression are shown in the heatmap. Value of each sample represent the average of normalized FPKM three replications. Low expression of genes is shown in green rectangle and high expression is shown in red rectangle. **b** qRT-PCR was used to verify the expression levels of randomly selected effector genes. The different letter denote significant differences with $P < 0.05$. L8, L24, and L48 represent leaf-infected samples. P8, P24, and P48 are panicle-infected samples, respectively

of *M. oryzae* on panicle tissue. We have sequenced a genome-wide transcriptome during *M. oryzae* infection on early infected tissues using stranded RNA sequencing approach. Genes expressing differentially at leaf and neck infection stages will help to study dual epidemics. It will also help plant breeders to utilize these genes to develop blast disease resistance rice in a region-specific manner. Meanwhile, it is indicative for changes in gene signaling when pathogen invasion shifts from leaf infection to other tissue like neck and panicle.

In this study, we employed the RNA-seq technique to study gene expression pattern during rice-*M. oryzae* interaction at the leaf and panicle infection stages. The transcriptome assays for the non-infected and infected tissues of leaf and neck revealed the contrasting gene expression profile. By comparing the DEGs from three leaf and panicle tissues at 8, 24, and 48 hpi, we found that genes were differentially expressed in different tissues (Additional file 1: Table S2 and Additional file 3: Table S3). Though the reads matching to *M. oryzae* genome is slight low, the data are overall

informative. We identified most DEGs induced at infection stage, which are consistent to previous reports. For example, CAZymes-coding gene MGG_02393 belonging to CE5 subfamily was found to be up-regulated as revealed by RNA-seq (Kawahara et al. 2012). The other gene MGG_09100 which encodes Cutinase 2 (Cut2), was also up-regulated at initial infection stage (Franck et al. 2013; Shimizu et al. 2019). In addition, our data support the expression patterns of known effectors, such as SLP1, BAS1, and MC69 (Dong et al. 2015).

GO enrichment analysis of DEGs revealed that DEGs were involved in three important processes (biological processes, cellular component, and molecular function) that were differentially enriched at the leaf and panicle infection stages (Fig. 3, Additional file 4: Table S4, and Additional file 5: S5). An interesting finding of pathway analysis of *M. oryzae* DEGs at leaf infection stage is the high expression of genes related to metabolism pathways. However, we found that genes involved in "Carbon metabolism" and "Ribosome" pathways were remarkably enriched in *M. oryzae* at panicle infection stage (Fig. 4 and Additional file 6: Table S6). These data revealed that infection-specific expression of genes in *M. oryzae* are involved in different functional processes and pathways.

Researches of leaf blast contributed to understand infection mechanism of *M. oryzae* in seedling stage. However, the study of neck blast is limited, and the information acquired from leaf blast may not be applicable to other infection types like nodal blast, panicle blast, and neck blast. How are the DEGs associated with the spatiotemporal interaction between *M. oryzae* and rice leaf or panicle? The gene expression pattern largely depends on different plant tissues and the *M. oryzae* strains (Mahesh et al. 2021). Due to the same genetic background of pathogen at leaf and panicle stages, we speculated that the difference might depend on molecular mechanisms between rice leaf or panicle and *M. oryzae* interactions. In other plant pathogens, many pathogenic-related genes were reported for some tissue-specific infection pathogens. As we all know, the ascomycete fungus *Ustilaginoidea virens* causes rice false smut (RFS), a unique floret disease. Functional genomics and transcriptome analyses predict that more than 1000 genes are involved in the virulence and pathogenicity of *U. virens* (Yu et al. 2023). These putative virulence factors are closely related to the pathways that have been identified to be implicated in *U. virens* pathogenicity, mycelial growth, conidiation, and stress tolerance. In *Fusarium graminearum*, Wanjiru and colleagues (Mary Wanjiru et al. 2002) showed that the pathogenicity of *F. graminearum* is dependent on the extracellular secreting enzymes. The fungus invades the host via the epidermis, leading to the destruction of the host's cellulose, pectin, and xylan. Further research indicated that the *F. graminearum* Gpmk1 MAP kinase regulates the induction of extracellular endoglucanase, xylanolytic, as well as proteolytic activities (Jenczmionka & Schäfer 2005). In our study, we found that many genes involved in signal pathways, secondary metabolism, and transcriptional regulation pathways exhibited transcriptional differences between leaf and panicle stages (Additional file 2: Table S2 and Additional file 3: Table S3).

It is known that fungi constantly produce several CAZymes to degrade cell wall polysaccharides during infection. Leaf-infecting fungi often breach the hard waxy cuticle that coats aerial plant structures (Mendgen & Deising 1993; Gómez Luciano et al. 2019). Identification of CAZymes-coding genes in *M. oryzae* showed that CE, CBM, and GH families may play diverse roles in the degradation of plant cuticles at the leaf infection stage. MGG_02393, a CE5 subfamily gene, was found to be up-regulated (Kawahara et al. 2012), and MGG_09100 (Cutinase 2, Cut2) was also up-regulated at 12 hpi and down-regulated at 36 hpi (Franck et al. 2013; Shimizu et al. 2019). Our data are consistent with the previous reports. These CAZymes-coding genes are required for *M. oryzae* to sense the host tissues and to initiate differentiation, penetration, and full virulence. However, there are limited reports showing the relevance of CAZymes of *M. oryzae* at neck infection stage. Contrast to DEGs in *M. oryzae* at leaf infection stage, our findings indicate that GT and GH families may play an important role in *M. oryzae* during rice panicle infection. Taken together, the CAZymes CE, GH, and CBM families play essential roles during the attacks of *M. oryzae* on rice leaf, but GT and GH family of *M. oryzae* may act in rice panicle infection.

Effectors are secreted proteins by *M. oryzae* that often target plant immune system to suppress host defense and, as a result they contribute to the proliferation of the pathogen (Jones & Dangl 2006; Lo Presti et al. 2015). During infection, pathogens secrete effectors as biological weapons to help invade and propagate in host plants by targeting hosts' physical barriers for disruption, where they create conducive conditions for invasion and proliferation. As the result, they disturb host cell physiological activity and dampen plant downstream immune responses. Therefore, it is essential to analyze the virulence of effectors at leaf and panicle infection stages. Figure 6 shows that most known effector are conserved during leaf and panicle infection processes. Further BLASTP analysis found that *BAS2*, *BAS3*, *BAS113*, *BAS162*, *MoCDIP4*, and *MoHEG13* have different numbers of homologous genes. We found that effectors and their homologous exhibited different expression levels. Taking an example of effector *BAS3*, it has higher expression levels at leaf infection and panicle infection stages,

but its homologous gene MGG_16415 was significantly increased about 6-fold to 50-fold at panicle infection stages. Another effector *MoHEG13* (MGG_09378) and its homologous gene MGG_17582 both exhibited higher expression levels at leaf infection and panicle infection stages, but their homologous gene MGG_17319 only displayed higher expression level at L8 stage. Therefore, these data suggest that homologous genes might be involved in the different infection mechanisms of *M. oryzae,* in order to suppress host defense during leaf and panicle infection processes.

Conclusions

We performed a comparative analysis to investigate transcriptome of *M. oryzae* at leaf and panicle infection stages. The data showed that CAZymes CE, CBM, and GH families may play an important role during *M. oryzae* infection on rice leaf. However, GT and GH families may play important roles in *M. oryzae* infection rice panicle. Further analysis of effectors and their homologous proteins indicate that they may be involved in different mechanisms for *M. oryzae* that help to suppress host defense during leaf and panicle infection. Our results provide resources to characterize their functions in future. It is assumed that there are differential genes expressed in pathogen at different plant tissues due to the different set of defense and pathogenicity related arsenals deployed by plants. The infection-specific transcriptome data presented in this study will help to elucidate the molecular mechanism of *M. oryzae* during leaf and panicle infection.

Methods

Plant and fungal materials, growth conditions, and treatments

Seeds of rice cultivar Nipponbare (Nip) were surface sterilized, germinated, and grown in a greenhouse (26 ± 2°C and 16 h light/8 h dark). For pathogen inoculation, *M. oryzae* was maintained on complete media (CM) (6 g yeast extract, 6 g casamino acids, and 10 g of sucrose per litre) at 28°C. Later, they were transferred to straw decoction and corn media (SDC) (100 g straw, 40 g corn powder, 15 g agar in 1 L distilled water) and kept under 28°C for 7 days for reproductive growth. Then, they were grown under constant fluorescent light (YZ 36W T8 12, Xiguang, China) for 3 days. Conidia were harvested from the 7-day-old SDC medium, and dissolved them in sterile distilled water, and the concentration was adjusted after filtration through three layers of Miracloth (CalBiochem) (Zhang et al. 2011; Du et al. 2013).

For rice leaf infection assays, three-week-old rice plants were used for inoculation with *M. oryzae* strain Guy11 at 1×10^6 conidia/mL. For rice panicle infection assays, conidial suspensions were injected into the rice sheath at the heading stage (Du et al. 2021a). Finally, the tissues were collected at 8, 24, and 48 hpi after inoculation. Three replicates were taken at each infection time point and the tissues were prepared for transcriptome sequencing.

RNA library preparation, Illumina sequencing, and analysis of the reads

The library for RNA sequencing was prepared using Illumina True-Seq RNA Library Prep Kit (San Diego, California, USA) by following the manual. Each biological replicate was a pool of five independent panicles. Three biological replicates were used for each sample and thus 19 samples (three replicates for each infection time point and a conidia sample used as control) were sequenced. Illumina NovaSeq 6000 platform was used to generate large amounts of sequencing data performing paired-end sequencing runs using more than 1 μg total RNA (RNA integrity number, RIN > 7) to obtain 150 bp sequence length reads. The raw reads were processed using the bioinformatics analysis platform BMKCloud (www.biocloud.net). Quality analysis of raw reads was further subjected to quality check by FastQC software (Andrews 2010). Finally, raw data is processed to obtain clean data using the BMKCloud platform.

Normalization of expression levels of genes from RNA-seq and gene annotation

All the clean reads were mapped to the reference genome of *M. oryzae* 70–15 (https://www.ncbi.nlm.nih.gov/datasets/genome/GCF_000002495.2/) using TopHat version 2.1.1 with default parameters (Trapnell et al. 2009). The expression level of a gene from RNA-seq was normalized using Fragments Per Kilobase of exon model per Million mapped fragments (FPKM) method (Mortazavi et al. 2008). Gene annotation, including gene ontology (GO) and Kyoto Encyclopedia of Genes and Genomes (KEGG) annotations, was referred by (Zhang et al. 2014).

Identification of DEGs of *M. oryzae* at infection stage

The gene expression analysis between *M. oryzae*-inoculated and conidia (control) samples was performed using the DESeq2 R package (1.16.1) (Anders & Huber 2010). Genes with a combination of P value < 0.01 and the absolute value of $|\text{Log}_2$ fold change$| \geq 1.5$ were regarded as DEGs. For grouping DEGs with similar expression patterns, a hierarchical clustering was generated using the expression values from each library (Liang et al. 2022). Analysis was conducted using Cluster 3.0 software with Pearson correlation as the distance measure. The cluster tree contained distinct clusters, which include genes with a unique expression profile by visual inspection.

Quantitative real time PCR (qRT-PCR)

Total RNA was extracted and purified by Qiagen RNAeasy Mini kit (Qiagen Inc., Valencia, CA, United States). RNA isolation was performed, and cDNA synthesis was carried out using the Superscript IV Reverse transcriptase cDNA synthesis kit (TB Green® Premix Ex Taq™ II). All cDNA samples were diluted to 20/ng prior to qRT-PCR. qRT-PCR was run on an ABI 7500 Real-Time PCR System (Applied Biosystems, Foster City, CA, USA) following the manufacturer's instructions. Reactions were performed in a 20 µL volume containing 10 µL of SYBR premix Ex Taq (SYBR Prime Script RT-PCR kit; TaKaRa), 0.4 µL of ROX reference dye (SYBR Prime Script RT-PCR kit; TaKaRa), 2 µL of cDNA template (50 ng), 0.4 µL of each primer (10 mM), and 6.8 µL of sterile distilled water. Transcripts of genes were analyzed and the *ACTIN* gene (MGG_03982) was used as an internal control. The amplification conditions for the reactions were 95°C for 3 min, with 25 cycles of 95°C for 30 s, followed by 55°C for 30 s, 72°C for 30 s and fluorescence read at 72°C at the end of each cycle. The 'Ct' values were normalized based on 'Ct' value of reference genes and differential gene expression (fold change) was calculated as per $2^{-\Delta\Delta Ct}$ method. qRT-PCR was repeated in triplicate with three independent biological experiments, and the primer pairs used are listed in Additional file 10: Table S10.

Abbreviations

AAs	Auxiliary activities
CAZymes	Carbohydrate-active enzymes
CBMs	Carbohydrate-binding modules
CEs	Carbohydrate esterases
CM	Complete media
CWDEs	Cell wall degrading enzymes
DEGs	Differentially expressed genes
FPKM	Fragments Per Kilobase of exon model per Million mapped fragments
GHs	Glycoside hydrolases
GO	Gene ontology
GTs	Glycosyltransferases
HCL	The hierarchical clustering
hpi	Hour post-inoculation
KEGG	Kyoto Encyclopedia of Genes and Genomes
Nip	Nipponbare
PLs	Polysaccharide lyases
qRT-PCR	Quantitative Real-time PCR
RNA-seq	RNA-seq sequencing
RFS	Rice false smut
SDC	Straw decoction and corn

Supplementary Information

The online version contains supplementary material available at https://doi.org/10.1186/s42483-024-00248-7.

Additional file 1: Table S1. DEGs of *M. oryzae* at different infection stages compared to conidia.

Additional file 2: Table S2. DEGs analysis of *M. oryzae* at leaf infection processes compared to panicle infection processes.

Additional file 3: Table S3. DEGs analysis of *M. oryzae* at panicle infection processes compared to leaf infection processes.

Additional file 4: Table S4. GO enrichment analysis for *M. oryzae* DEGs during leaf infection process.

Additional file 5: Table S5. GO enrichment analysis for *M. oryzae* DEGs during panicle infection processes.

Additional file 6: Table S6. KEGG pathway enrichment analysis for *M. oryzae* DEGs.

Additional file 7: Table S7. CAZymes analysis of *M. oryzae* DEGs at leaf infection processes.

Additional file 8: Table S8. CAZymes analysis of *M. oryzae* DEGs at panicle infection processes.

Additional file 9: Table S9. Verified *M. oryzae* effectors and their homologues.

Additional file 10: Table S10. Primers used in this study.

Acknowledgements

Not applicable.

Authors' contributions

DY and LY conceived and designed the experiments. LD and QZ performed the experiments and analyzed the data. YJ, ZR, ST, YM, CH, PX, WS, QJ, and LY supervised the manuscript and provided guidance. The manuscript was written by DY. All authors read and approved the final manuscript.

Funding

This study was supported by the National Natural Science Foundation of China (32272508), Jiangsu Agricultural Science and Technology Innovation Fund (CX(19)1008), and the Revitalization Foundation of Seed Industry of Jiangsu (JBGS(2021)005).

Availability of data and materials

All data generated or analyzed during this study are included in this published article [and its supplementary information files].

Declarations

Ethics approval and consent to participate

Not applicable.

Consent for publication

Not applicable.

Competing interests

The authors declare that they have no competing interests.

Received: 28 December 2023 Accepted: 23 April 2024
Published online: 20 June 2024

References

Agrios G, Plant Pathology Academic Press San Diego. Plant pathology. 4th ed. San Diego: Academic Press; 1997.
Anders S, Huber W. Differential expression analysis for sequence count data. Genome Biol. 2010;11:R106.
Andrews S. FastQC: a quality control tool for high throughput sequence data. 2010. https://www.bioinformatics.babraham.ac.uk/projects/fastqc/.
Balal MS, Selim AK, Hassanien SH, Maximoos MA. Inheritance of resistance to leaf and neck blast in rice. Egypt J Genet Cytol. 1977;6(2):332–41.
Buchfink B, Xie C, Huson DH. Fast and sensitive protein alignment using DIAMOND. Nat Methods. 2015;12(1):59–60.

Dean RA, Talbot NJ, Ebbole DJ, Farman ML, Mitchell TK, Orbach MJ, et al. The genome sequence of the rice blast fungus *Magnaporthe grisea*. Nature. 2005;434(7036):980–6.
Dong YH, Ying L, Zhao MM, Jing MF, Liu XY, Liu MX, et al. Global genome and transcriptome analyses of *Magnaporthe oryzae* epidemic isolate 98–06 uncover novel effectors and pathogenicity-related genes, revealing gene gain and lose dynamics in genome evolution. PLoS Pathog. 2015;11(4):e1004801.
Du Y, Zhang HF, Hong L, Wang JM, Zheng XB, Zhang ZG, et al. Acetolactate synthases MoIlv2 and MoIlv6 are required for infection-related morphogenesis in *Magnaporthe oryzae*. Mol Plant Pathol. 2013;14(9):870–84.
Du Y, Qi ZQ, Liang D, Yu JJ, Yu MN, Zhang RS, et al. *Pyricularia* sp. *jiangsuensis*, a new cryptic rice panicle blast pathogen from rice fields in Jiangsu Province, China. Environ Microbiol. 2021a;23(9):5463–80.
Du Y, Qi ZQ, Yu JJ, Yu MN, Cao HJ, Zhang RS, et al. Effects of panicle development stage and temperature on rice panicle blast infection by *Magnaporthe oryzae* and visualization of its infection process. Plant Pathol. 2021b;70(6):1436–644.
Finn RD, Clements J, Eddy SR. HMMER web server: interactive sequence similarity searching. Nucleic Acids Res. 2011;39:W29–37.
Franck WL, Gokce E, Oh Y, Muddiman DC, Dean RA. Temporal analysis of the *Magnaporthe oryzae* proteome during conidial germination and cyclic AMP (cAMP)-mediated appressorium formation. Mol Cell Proteomics. 2013;12(8):2249–65.
Gómez Luciano LB, Tsai IJ, Chuma I, Chuma I, Tosa Y, Chen YH, et al. Blast fungal genomes show frequent chromosomal changes, gene gains and losses, and effector gene turnover. Mol Biol Evol. 2019;36(6):1148–61.
Hu ML, Luo LX, Wang S, Liu YF, Li JQ. Infection processes of *Ustilaginoidea virens* during artificial inoculation of rice panicles. Eur J Plant Pathol. 2014;139:67–77.
Jenczmionka NJ, Schäfer W. The Gpmk1 MAP kinase of *Fusarium graminearum* regulates the induction of specific secreted enzymes. Curr Genet. 2005;47:29–36.
Jeon J, Lee GW, Kim KT, Park SY, Kim S, Kwon S, et al. Transcriptome profiling of the rice blast fungus *Magnaporthe oryzae* and its host *Oryza sativa* during infection. Mol Plant Microbe Interact. 2020;33(2):141–4.
Jones JD, Dangl JL. The plant immune system. Nature. 2006;444:323–9.
Kawahara Y, Oono Y, Kanamori H, Matsumoto T, Itoh T, Minami E. Simultaneous RNA-seq analysis of a mixed transcriptome of rice and blast fungus interaction. PLoS One. 2012;7(11):e49423.
Khan MA, Bhuiyan MR, Hossain MS, Sen PP, Ara A, Siddique MA, Ali MA. Neck blast disease influences grain yield and quality traits of aromatic rice. CR Biol. 2014;337(1):635–41.
Kong LA, Li GT, Liu Y, Liu MG, Zhang SJ, Yang J, et al. Differences between appressoria formed by germ tubes and appressorium-like structures developed by hyphal tips in *Magnaporthe oryzae*. Fungal Genet Biol. 2013;56:33–41.
Liang D, Qi ZQ, Du Y, Yu JJ, Yu MN, Zhang RS, et al. Identification of differentially expressed genes reveal conserved mechanisms in the Rice-*Magnaporthe oryzae* Interaction. Front Plant Sci. 2022;13:723356.
Lo Presti L, Lanver D, Schweizer G, Tanaka S, Liang L, Tollot M, et al. Fungal effectors and plant susceptibility. Annu Rev Plant Biol. 2015;66:513–45.
Mahesh H, Shirke MD, Wang GL, Gowda M. In planta transcriptome analysis reveals tissue-specific expression of pathogenicity genes and microRNAs during rice-*Magnaporthe* interactions. Genomics. 2021;113(1):265–75.
Mary Wanjiru W, Zhensheng K, Buchenauer H. Importance of cell wall degrading enzymes produced by *Fusarium graminearum* during infection of wheat heads. Eur J Plant Pathol. 2002;108:803–10.
Mehrabi R, Zhao XH, Kim Y, Xu JR. The cAMP signaling and MAP kinase pathways in plant pathogenic fungi. Plant Relation (The Mycota V). 2009;5:157–72.
Mendgen K, Deising H. Infection structures of fungal plant pathogens-a cytological and physiological evaluation. New Phytol. 1993;124(2):193–213.
Mortazavi A, Williams BA, Mccue K, Schaeffer L, Wold B. Mapping and quantifying mammalian transcriptomes by RNA-Seq. Nat Methods. 2008;5(7):621–8.
Mosquera G, Giraldo MC, Khang CH, Coughlan S, Valent B. Interaction transcriptome analysis identifies *Magnaporthe oryzae* BAS1-4 as biotrophy-associated secreted proteins in rice blast disease. Plant Cell. 2009;21(4):1273–90.
Oh Y, Donofrio N, Pan H, Coughlan S, Brown DE, Meng S, et al. Transcriptome analysis reveals new insight into appressorium formation and function in the rice blast fungus *Magnaporthe oryzae*. Genome Biol. 2008;9(5):1–24.
Oliva R, Win J, Raffaele S, Boutemy L, Bozkurt TO, Chaparro-Garcia A, et al. Recent developments in effector biology of filamentous plant pathogens. Cell Microbiol. 2010;12(6):705–15.
Ou S, Nuque F. The relation between leaf and neck resistance to the rice blast disease. Int Rice Commonw Newsl. 1963;12:30–4.
Quoc N, Chau N. The role of cell wall degrading enzymes in pathogenesis of *Magnaporthe oryzae*. Curr Protein Pept Sci. 2017;18(10):1019–34.
Shimizu M, Nakano Y, Hirabuchi A, Yoshino K, Kobayashi M, Yamamoto K, et al. RNA-Seq of in planta-expressed *Magnaporthe oryzae* genes identifies *MoSVP* as a highly expressed gene required for pathogenicity at the initial stage of infection. Mol Plant Pathol. 2019;20(12):1682–95.
Soanes DM, Chakrabarti A, Paszkiewicz KH, Dawe AL, Talbot NJ. Genome-wide transcriptional profiling of appressorium development by the rice blast fungus *Magnaporthe oryzae*. PLoS Pathog. 2012;8(2):e1002514.
Trapnell C, Pachter L, Salzberg SL. TopHat: discovering splice junctions with RNA-Seq. Bioinformatics. 2009;25(9):1105–11.
Tucker SL, Besi MI, Galhano R, Franceschetti M, Goetz S, Lenhert S, et al. Common genetic pathways regulate organ-specific infection-related development in the rice blast fungus. Plant Cell. 2010;22(3):953–72.
Van Der Does HC, Rep M. Virulence genes and the evolution of host specificity in plant-pathogenic fungi. Mol Plant Microbe Interact. 2007;20(10):1175–82.
Yan X, Tang BZ, Ryder LS, MacLean D, Were VM, Eseola AB, et al. The transcriptional landscape of plant infection by the rice blast fungus *Magnaporthe oryzae* reveals distinct families of temporally co-regulated and structurally conserved effectors. Plant Cell. 2023;35(5):1360–85.
Yang C, Liu R, Pang J, Ren B, Zhou HB, Wang G, et al. Poaceae-specific cell wall-derived oligosaccharides activate plant immunity via OsCERK1 during *Magnaporthe oryzae* infection in rice. Nat Commun. 2021;12(1):2178.
Yin YB, Mao XZ, Yang JC, Chen X, Mao FL, Xu Y. dbCAN: a web resource for automated carbohydrate-active enzyme annotation. Nucleic Acids Res. 2012;40:W445–51.
Yu SW, Liu PW, Wang JY, Li DY, Zhao D, Yang C, et al. Molecular mechanisms of *Ustilaginoidea virens* pathogenicity and their utilization in disease control. Phytopathol Res. 2023;5(1):1–14.
Zerillo MM, Adhikari BN, Hamilton JP, Buell CR, Lévesque CA, Tisserat N. Carbohydrate-active enzymes in Pythium and their role in plant cell wall and storage polysaccharide degradation. PLoS One. 2013;8(9):e72572.
Zhang HF, Liu KY, Zhang X, Tang W, Wang JS, Guo M, et al. Two phosphodiesterase genes, PDEL and PDEH, regulate development and pathogenicity by modulating intracellular cyclic AMP levels in *Magnaporthe oryzae*. PLoS One. 2011;6(2):e17241.
Zhang Y, Peng LF, Wu Y, Shen YY, Wu XM, Wang JB. Analysis of global gene expression profiles to identify differentially expressed genes critical for embryo development in *Brassica rapa*. Plant Mol Biol. 2014;86:425–42.